Hindawi Publishing Corporation
Advances in Mechanical Engineering
Volume 2014, Article ID 690985, 12 pages
http://dx.doi.org/10.1155/2014/690985

Research Article

Nonintrusive-Polynomial-Chaos-Based Kinematic Reliability Analysis for Mechanisms with Mixed Uncertainty

Jianbin Guo,[1,2] Yao Wang,[2] and Shengkui Zeng[1,2]

[1] *Science and Technology on Reliability and Environmental Engineering Laboratory, Beijing 100191, China*
[2] *School of Reliability and Systems Engineering, Beihang University, Beijing 100191, China*

Correspondence should be addressed to Shengkui Zeng; zengshengkui@buaa.edu.cn

Received 7 March 2014; Revised 16 May 2014; Accepted 21 May 2014; Published 11 June 2014

Academic Editor: Jia-Jang Wu

Due to the scarcity of statistical data, epistemic uncertainties are inevitable in the mechanism. As a promising uncertainty quantification technique, polynomial chaos has advantages over other methods in terms of accuracy and efficiency. In this paper, an improved nonintrusive polynomial chaos method is proposed for the kinematic reliability analysis of the mechanism with fuzzy and random variables as well as fuzzy failure/safety states. Klir log-scale transformation is applied to unify the fuzzy and random variables. Meanwhile, the polynomial-chaos-based probability formula of the fuzzy event is developed to characterize the fuzzy failure/safety states. The proposed method is applied to the reliability analysis of a retractable mechanical system. The results show good accuracy and efficiency of the proposed method when compared with the response surface method (RSM), Kriging method, and Monte Carlo simulation (MCS).

1. Introduction

Computational dynamics model, which extends the classical mechanics into the multibody formalisms and computer algorithms, is always applied to the investigation of complicated kinematic outputs of mechanisms [1]. Kinematic reliability is defined as the probability that the position and/or orientation of the mechanism output remain within a specified range of the desired position and/or orientation [2–4]. In order to evaluate the kinematic reliability, uncertainty should be propagated through the computational dynamics model. The uncertainty propagation requires the numerical solution of numerous high-order and nonlinear algebraic and differential equations. Therefore, it is very time-consuming to apply the crude MCS to quantify the uncertainty, especially when the clearances of joints are considered in the computational dynamics model.

Many surrogate models, such as RSM, kriging method, and artificial neural networks (ANN), have been developed to improve the efficiency of the uncertainty quantification. Among these surrogate model methods, polynomial chaos expansion (PCE) is a technique that uses a polynomial-based stochastic space to represent and propagate uncertainty [5]. It can be mathematically explained as the projection of the stochastic process to the probability space. The polynomials are the basis vectors of the probability space, and the coefficients of PCE are the coordinates of the stochastic process. Compared to the conventional surrogate models, it is more accurate and efficient. Moreover, PCE converges to any stochastic processes with finite second-order moments [6].

PCE can be divided into intrusive approaches and nonintrusive approaches. Intrusive approaches calculate the unknown polynomial coefficients by projecting the resulting equations onto basis functions, which require the modification of the deterministic code. Thus they are difficult, expensive, and time-consuming for many complex computational problems [7]. On the contrary, in the nonintrusive approaches, simulations are used as black boxes, and the sampling-based methods are usually employed to calculate the PCE coefficients. Nonintrusive polynomial chaos (NIPC) is easier to execute and thus more applicable to the kinematic reliability analysis.

Uncertainties exist in the analysis and design of mechanisms can be divided into aleatory uncertainty and epistemic uncertainty [8, 9]. Aleatory uncertainty is considered to be irreducible variability inherent in the mechanisms. It is usually described by probability. Epistemic uncertainty is a potential inaccuracy due to the lack of knowledge [10]. Epistemic uncertainty sources in mechanisms usually include (1) the epistemic uncertainty of parameters due to the small sample size of the products and the scarcity of the test data and (2) the epistemic uncertainty of the failure/safety state due to the vagueness in the failure criteria. And possibility theory is a powerful tool to measure the epistemic uncertainty. However, probability and possibility are defined in different measure spaces. As previously mentioned, PCE is a projection in the probability space on the basis of polynomial chaos. Therefore, conventional PCE methods cannot tackle the uncertainty quantification with both fuzzy variables and random variables.

In the research of PCE-based mixed uncertainty quantification, Eldred [5] proposed an improved second-order probability (SOP) method, in which a nested iteration is employed. PCE is used to quantify the randomness in the inner loop to obtain the cumulative distribution function. And optimization-based interval estimation is applied to calculate the maximum and minimum value of the system responds. The system responses are finally expressed in an interval form. Monti et al. [11] presented a framework of uncertainty quantification by PCE, in which all of the epistemic uncertainty is described by interval. Fuzzy variables in the system are extended into the random fuzzy variables, where a combination of alpha-cuts provides the confidence level related to the probabilistic part and the nonprobabilistic part of the uncertainty.

However, things are more complicated for the kinematic reliability analysis and design. In the real engineering problem, in addition to the epistemic parameter uncertainties, there are also epistemic uncertainties in the failure/safety states due to the vagueness in the failure criteria of mechanisms. Since PCE-based approaches mentioned above are unable to deal with the coexistence of the fuzzy failure/safety states and the fuzzy/random variables in the mechanical system, this paper proposes an NIPC-based method to evaluate the kinematic reliability of the mechanism with the fuzzy and random variables as well as the fuzzy failure/safety state. Klir log-scale transformation is employed to unify the fuzzy and random variables. The fuzzy failure/safety state is characterized by the fuzzy probability theory. And the polynomial-chaos-based probability formula of the fuzzy event is used to calculate the kinematic reliability. The results of the kinematic reliability analysis for a retractable mechanism show the accuracy and efficiency of the proposed method.

The paper is structured as follows. In Section 2 the theory of the polynomial chaos and the Point-Collocation method is reviewed. In Section 3 the representation of epistemic uncertainty in the mechanism is discussed. In Section 4 the theory, algorithm, and procedure of the proposed NICP method are presented. The proposed method is applied to a retractable mechanical system in Section 5 and conclusions are drawn in Section 6.

Table 1: Optimality of the polynomial basis functions corresponding to the standard forms of probability distributions.

Distribution	Polynomial basis function	Support range
Normal	Hermite	$[-\infty, \infty]$
Uniform	Legendre	$[-1, 1]$
Beta	Jacobi	$[-1, 1]$
Exponential	Laguerre	$[0, \infty]$
Gamma	Generalized Laguerre	$[0, \infty]$

2. Polynomial Chaos Theory

PCE is a stochastic method that was first introduced by Wiener as "Homogeneous Chaos" [12]. The theory evolved into the Wiener-Askey polynomial chaos which includes the entire Askey scheme of orthogonal polynomials [6]. Recently, PCE has become a research hotspot in the uncertainty quantification [13–15].

System response G can be represented by PCE as

$$G(\boldsymbol{\xi}) = a_0 + \sum_{i_1=1}^{\infty} a_{i_1} \Gamma_1 \left(\xi_{i_1}\right) + \sum_{i_1=1}^{\infty} \sum_{i_2=1}^{i_1} a_{i_1 i_2} \Gamma_2 \left(\xi_{i_1}, \xi_{i_2}\right) + \sum_{i_1=1}^{\infty} \sum_{i_2=1}^{i_1} \sum_{i_3=1}^{i_2} a_{i_1 i_2 i_3} \Gamma_3 \left(\xi_{i_1}, \xi_{i_2}, \xi_{i_3}\right) + \cdots, \tag{1}$$

where a_i is the coefficient of the PCE and $\Gamma_n(\xi_{i_1}, \ldots, \xi_{i_n})$ is the selected polynomial basis function with the freedom of n. The polynomials are orthogonal because the inner product of each two of them is zero. ξ_{i_1} is the random variable with specific distribution that determines the polynomial basis function. The optimality of these basis functions selections derives from their orthogonality with respect to weighting functions that correspond to the PDFs of the continuous distributions when placed in a standard form [5]. According to Askey scheme, the linkage between standard forms of continuous probability distributions and polynomial bases is shown in Table 1.

As the parameter uncertainty follows the standard normal distribution, the basis function ideally takes the form of Hermite polynomial. Thus $\Gamma_n(\xi_{i_1}, \ldots, \xi_{i_n})$ can be described by

$$\Gamma_n \left(\xi_{i_1}, \ldots, \xi_{i_n}\right) = (-1)^n e^{(1/2)\boldsymbol{\xi}^T \boldsymbol{\xi}} \frac{\partial^n}{\partial \xi_{i_1} \cdots \partial \xi_{i_n}} e^{-(1/2)\boldsymbol{\xi}^T \boldsymbol{\xi}}, \tag{2}$$

where $\boldsymbol{\xi}$ is the vector of the standard normal random variables. In practice, there are finite random variables in PCE. Thus (1) can be shown in a compact form with a product of one-dimensional Hermite polynomials. Consider

$$G(\boldsymbol{\xi}) = \sum_{j=0}^{N_a - 1} a_j \Psi_j (\boldsymbol{\xi}), \tag{3}$$

where

$$\Psi_j (\boldsymbol{\xi}) = \prod_{i=1}^{n} \psi_{m_i^j} \left(\xi_i\right) = \Gamma_n \left(\xi_{i_1}, \ldots, \xi_{i_n}\right). \tag{4}$$

The total number of terms in the PCE of order p including n random variables is given by

$$N_a = 1 + \frac{n!}{(n-1)!} + \frac{(n+1)!}{(n-1)!2!} + \cdots + \frac{(n-1+p)!}{(n-1)!p!} = \frac{(n+p)!}{n!p!}. \tag{5}$$

Point-Collocation NIPC method is first proposed by Walters [16] to approximate the polynomial chaos coefficients of a stochastic heat transfer problem. Hosder et al. [17] applied the Point-Collocation method (PCM) to stochastic fluid dynamics problems with geometric uncertainty. PCM calculates the coefficients of PCE through the evaluation of the system responses at collocation points. Hosder et al. [7] have observed that using a number of collocation points that are twice the total number of the coefficients gives a better approximation to the statistics at each polynomial degree. The coefficients can be calculated by PCM as follows:

$$\begin{bmatrix} G(\xi_1) \\ G(\xi_2) \\ \vdots \\ G(\xi_q) \end{bmatrix} = \begin{bmatrix} 1 & \Psi_1(\xi_1) & \cdots & \Psi_{N_a-1}(\xi_1) \\ 1 & \Psi_1(\xi_2) & \cdots & \Psi_{N_a-1}(\xi_2) \\ \vdots & \vdots & \ddots & \vdots \\ 1 & \Psi_1(\xi_q) & \cdots & \Psi_{N_a-1}(\xi_q) \end{bmatrix} \begin{bmatrix} a_0 \\ a_1 \\ \vdots \\ a_{N_a-1} \end{bmatrix}, \tag{6}$$

where $\boldsymbol{\xi}_j$ is the vector of the jth set of the collocation points. In total, q ($q = 2N_a$) sets of collocation points are required. Equation (6) is a linear system of equations that can be solved by least squares method. The coefficients of PCE can be calculated as

$$\mathbf{a} = \left(\Pi^T \Pi\right)^{-1} \Pi^T \cdot G, \tag{7}$$

where Π represents

$$\begin{bmatrix} 1 & \Psi_1(\xi_1) & \cdots & \Psi_{N_a-1}(\xi_1) \\ 1 & \Psi_1(\xi_2) & \cdots & \Psi_{N_a-1}(\xi_2) \\ \vdots & \vdots & \ddots & \vdots \\ 1 & \Psi_1(\xi_q) & \cdots & \Psi_{N_a-1}(\xi_q) \end{bmatrix} \tag{8}$$

and G represents the vector

$$\begin{bmatrix} G(\xi_1) \\ G(\xi_2) \\ \vdots \\ G(\xi_q) \end{bmatrix}. \tag{9}$$

3. Epistemic Uncertainty Representation

3.1. Epistemic Uncertainty in Parameters. Epistemic uncertainty often exists in the parameters of the mechanism due to kinematic unevenness caused by the scarcity of data [18]. Possibility theory is a powerful tool to measure the epistemic uncertainty in parameters [19]. And it is an extension of fuzzy set and fuzzy logic, which can be used to model uncertainties when there is little information or sparse data [20]. In possibility theory, the membership function is extended to possibility distribution. The subjective knowledge of the uncertain variable x can be represented with a pair (χ, r), where χ is the set of possible values for x and r is a function defined on χ. The function r provides a measure of confidence that is assigned to each element of χ and is defined as the possibility distribution function for x. Possibility for a subset u of χ is defined by

$$\pi(u) = \sup\{r(x) : x \in u\}, \tag{10}$$

where $r(x)$ is required to meet the following conditions:

$$\begin{gathered} \sup\left(r(x) : x \in \chi\right) = 1 \\ 0 \le r(x) \le 1 \quad x \in \chi. \end{gathered} \tag{11}$$

3.2. Epistemic Uncertainty in the Failure/Safety State. The kinematic reliability is always related with the failure criteria. Since failure criteria are determined by customers or experts, and sometimes these subjective failure criteria cannot be precisely defined in a reasonable way, the binary failure/safety state assumption is not applicable [21]. The vagueness in the failure criteria leads to the epistemic uncertainty in the failure/safety state. Meanwhile, randomness is also presented in the failure/safety state for the stochastic characteristic of the system response. In summary, both vagueness and randomness exist in the failure/safety state of mechanisms.

Fuzzy probability theory is an extension of probability theory to deal with mixed aleatory/epistemic uncertainty [22]. The fuzzy probabilistic model is settled between the probabilistic uncertainty model and nonprobabilistic uncertainty models. It treats the elements of a population not as crisp quantities but as set-valued quantities in an imprecise manner [23].

In the analysis of the kinematic reliability, the failure/safety state is interpreted as a fuzzy event Z which has a membership function determined by experts and customers. The common membership functions of the fuzzy failure/safety state, which is proved to be simple, effective and reliable [18], are shown in Figure 1.

(1) Trapezoid function

$$\mu_Z(g) = \begin{cases} \dfrac{g-a}{b-a} & a \le g < b \\ 1 & b \le g \le c \\ \dfrac{d-g}{d-c} & c < g \le d \\ 0 & \text{otherwise.} \end{cases} \tag{12}$$

(2) Combinational normal function

$$\mu_Z(g) = \begin{cases} e^{-kg^2} & g < a \\ 1 & a \le g \le b \\ e^{-kg^2} & g > b. \end{cases} \tag{13}$$

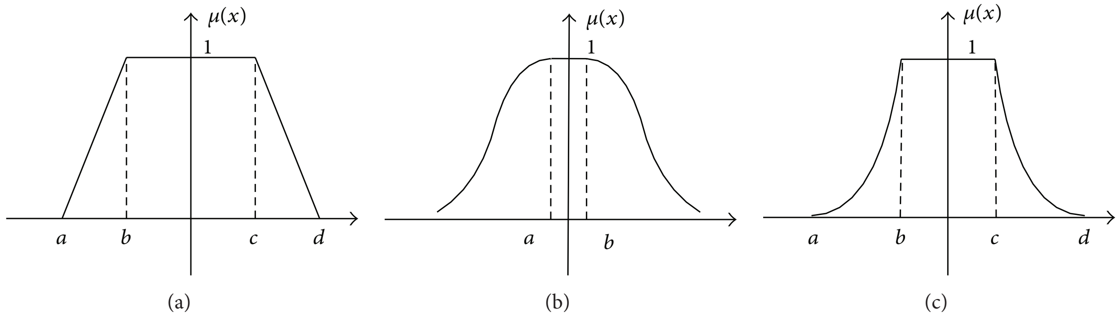

FIGURE 1: Three common membership functions: (a) Trapezoid function, (b) Combinational normal function, (c) Combinational ridge function.

(3) Combinational ridge function

$$\mu_Z(g) = \begin{cases} \frac{1}{2} + \frac{1}{2}\sin\frac{\pi}{b-a}\left(g - \frac{a+b}{2}\right) & a \le g < b \\ 1 & b \le g \le c \\ \frac{1}{2} + \frac{1}{2}\sin\frac{\pi}{c-d}\left(g - \frac{c+d}{2}\right) & c < g \le d \\ 0 & \text{otherwise.} \end{cases} \quad (14)$$

In (12) to (14), a, b, c, d are parameters of these membership functions, which is determined according to the limited data, the mission requirements, and the expertise; g is the actual motion output of the mechanism and $\mu_Z(g)$ is the fuzzy membership of the output g to the safety state.

4. NIPC-Based Kinematic Reliability Analysis Method

Since both fuzzy and random variables exist in the design process of mechanisms, NIPC is applied to quantify the mixed-uncertainty. The PC formula (3) can be rewritten as

$$G(\boldsymbol{\xi}, \mathbf{v}) = \sum_{j=0}^{N_a-1} a_j \Psi_j(\boldsymbol{\xi}, \mathbf{v}), \quad (15)$$

where $\mathbf{v}$ is the vector of fuzzy variables. Because NIPC is a projection in the probability space on the basis of Hermite polynomials, it requires transforming fuzzy variables into standard normal variables to unify the fuzzy and random variables.

4.1. Klir Log-Scale Transformation. On the transformation between the probability and the possibility, some meaningful principles are followed, so that the transformation is not arbitrary under these constraints. These principles include the following.

(1) The principle of possibility/probability consistency which formulates some conditions under which the probability and the possibility distributions are considered to be consistent [20].

(2) The principle of insufficient reason which is used to preserve the uncertainty of choices between outcomes [24].

(3) The principle of information invariance which starts from the viewpoint that the concept of uncertainty is intuitively connected with information [25].

(4) The principle of preference preservation which means that if an element is preferred over another element according to possibility distribution, then this preference is maintained in the probabilistic setting [26].

In engineering design, the ratio scale is widely used in the transformation between possibility and probability [27, 28]. It consists only of normalization of the data. Thus its advantage is the simplicity to be realized. The ratio scale in the discrete form is presented as

$$\pi(s_i) = \frac{p(s_i)}{\max[p(s_i)]}$$
$$p(s_i) = \frac{\pi(s_i)}{\sum \pi(s_i)}, \quad (16)$$

where $\pi(s_i)$ is the possibility of the element s_i; $p(s_i)$ is the probability of the element s_i. However, the ratio scale has poor performance in the compliance of some principles mentioned above [26]. It is too rigid to apply the ratio scale to the transformations between probability and possibility.

Through the comparison of the most common probability/possibility transformations found in the literature, Oussalah [26] proved that Klir log-scale transformation performs very well in the compliance of all the above mentioned principles. Klir log-scale transformation is created according to the principle of information invariance [29]. It keeps the Shannon entropy of the probabilistic uncertainty and the possibilistic uncertainty unchanged after the transformation. Thus this paper adopts the Klir log-scale transformation to unify the fuzzy and random variables. Klir log-scale transformation in the discrete form is presented as

$$\pi(s_i) = \beta \cdot p(s_i)^{\alpha}$$

$$\begin{aligned}-\sum_{i=1}^{n} p(s_i) \cdot \log_2 p(s_i) &= \sum_{i=2}^{n} \pi(s_i) \log_2 \left(\frac{i}{i-1}\right) \\ &\quad - \sum_{i=1}^{n-1} (\pi(s_i) - \pi(s_{i+1})) \log_2 \left(1 - i \cdot \sum_{j=i+1}^{n} \frac{\pi(s_j)}{j(j-1)}\right),\end{aligned} \tag{17}$$

where $\pi(s_i)$ and $p(s_i)$ are the possibility and probability of element s_i, respectively, which are both presented in a descend form.

Compared to the ratio scale transformation, the advantage of Klir log-scale transformation is that the amount of uncertainty and information is preserved under the transformations. It is also more excellent to satisfy other transformation principles. Nevertheless, it is difficult to obtain the parameters of the Klir log-scale transformation. Numerical solution is required to be solved to search the proper values of α and β. This paper presents an optimization algorithm to obtain the value of α and β. The optimization formulation is written as

$$\begin{aligned}\text{find} \quad & \alpha \\ \min \quad & |L+T| \\ \text{s.t.} \quad & p(s_i) = \frac{[\pi(s_i)]^{1/\alpha}}{\sum_{k=1}^{n} [\pi(s_k)]^{1/\alpha}} \\ & L = \sum_{i=1}^{n} p(s_i) \cdot \log_2 p(s_i) \\ & T = \sum_{i=2}^{n} \pi(s_i) \log_2 \left(\frac{i}{i-1}\right) \\ & \qquad - \sum_{i=1}^{n-1} (\pi(s_i) - \pi(s_{i+1})) \\ & \qquad \times \log_2 \left(1 - i \cdot \sum_{j=i+1}^{n} \frac{\pi(s_j)}{j(j-1)}\right).\end{aligned} \tag{18}$$

This optimization problem can be solved by sequential quadratic programming (SQP) which considers both of the accuracy and the convergence rate.

After being transformed from possibility to probability, uncertain parameters would follow nonstandard distributions. To convert these arbitrary random variables into the standard normal random variables, the series approximation is performed, which is under the assumption that an arbitrary random variable can be represented by a series expansion of the standard normal random variable. The series expansion is written as follows:

$$s = b_0 + b_1\xi + b_2\xi^2 + \cdots + b_n\xi^n, \tag{19}$$

where s represents the arbitrary random variable, ξ represents the standard normal random variable, and b_i is the unknown coefficient. The order of the expansion n is determined by the desired accuracy. The moments of the random variable s are computed by its probability distribution which has been obtained through the Klir log-scale transformation. Because the moments of the two sides of (19) should be equal, a linear system of equations is constructed so that the coefficients of the series expansion can be calculated. Then the relationship of the fuzzy variable and the standard normal variable is known. Consider

$$v \xrightarrow{\text{Klir log-scale transformation}} s \xrightarrow{\text{Series approximation method}} \tilde{\xi}. \tag{20}$$

The unification of fuzzy variables and random variables is realized by the Klir log-scale transformation and the series approximation method. In this way, the NIPC can be employed to approximate the motion output of the mechanism. Equation (15) is then rewritten as

$$G(\boldsymbol{\xi}, \tilde{\boldsymbol{\xi}}) = \sum_{j=0}^{N_a-1} a_j \Psi_j (\boldsymbol{\xi}, \tilde{\boldsymbol{\xi}}). \tag{21}$$

4.2. NIPC-Based Kinematic Reliability Analysis. The motion error function of the mechanism is given by

$$g(\mathbf{x}, \mathbf{v}) = \phi(\mathbf{x}, \mathbf{v}) - \phi_d, \tag{22}$$

where $\mathbf{x}$ is the vector of random variables; $\mathbf{v}$ is the vector of fuzzy variables; $\phi(\mathbf{x}, \mathbf{v})$ is the actual motion output which is obtained by the computational dynamics model since the structure of the mechanism is complicated, and ϕ_d is the desired motion output.

After the transformation of fuzzy variables and NIPC is performed to approximate the motion output of the mechanism, (22) can be presented as

$$g(\mathbf{x}, \mathbf{v}) = \hat{\phi}(\boldsymbol{\xi}, \tilde{\boldsymbol{\xi}}) - \phi_d, \tag{23}$$

where $\hat{\phi}(\boldsymbol{\xi}, \tilde{\boldsymbol{\xi}})$ is the approximated motion output obtained by NIPC.

To ensure that the mechanism works properly, the motion error should be less than an allowable error ε. Thus the event that the mechanism is in the safety state reads as

$$Z = \{|g(\mathbf{x}, \mathbf{v})| \le \varepsilon\} = \{|\hat{\phi}(\boldsymbol{\xi}, \tilde{\boldsymbol{\xi}}) - \phi_d| \le \varepsilon\}. \tag{24}$$

The kinematic reliability of the mechanism can be obtained as follow:

$$R_k = P\{Z\} = P\{|g(\mathbf{x}, \mathbf{v})| \le \varepsilon\}. \tag{25}$$

Since vagueness exists in the safety state, the event that the motion error belongs to the safety state is a fuzzy event. In this situation, the probability formula of the fuzzy event, which is a significant basis to the fuzzy probability theory, can be employed to calculate the kinematic reliability:

$$R_k = P(Z) = \int_{-\infty}^{+\infty} \mu_Z(g)\, p(g)\, dg, \tag{26}$$

where g is the motion error of the mechanism; $\mu_Z(g)$ is the membership function which is used to decide the membership that the motion error belongs to the fuzzy safety state Z; $p(g)$ is the probability density function of the motion error. Since the error function by NIPC approximation is explicit and simple, (26) can be solved by MCS.

The algorithm to evaluate the kinematic reliability is developed and shown as follows.

Step 1. In total, N sets of random numbers that follow the standard normal distribution are generated and brought into (21) to obtain the approximate motion outputs.

Step 2. The approximated motion outputs are then brought into (23) to compute the corresponding motion errors g_i ($i = 1, 2, \ldots, N$).

Step 3. The motion error g_i is carried into the membership function of the safety state to calculate its membership $\mu_Z(g_i)$.

Step 4. The approximated kinematic reliability is the mean of these memberships calculated according to the following equation:

$$R_k \approx \frac{1}{N}\sum_{i=1}^{N} \mu_Z(g_i). \tag{27}$$

The accuracy of the approximated kinematic reliability depends on the accuracy of the NIPC and the total sampling number N. The sampling number can be taken as a big value for the simple polynomial function of the PCE approximation. Therefore, it requires little solution time and the accuracy of the approximated kinematic reliability can be relatively high. The accuracy and efficiency of the proposed method would be demonstrated in the case study.

4.3. Procedure of the Method. The proposed NIPC-based kinematic reliability analysis method is employed to quantify the mixed uncertainty in the computational dynamics model. Then the kinematic reliability of the mechanism with fuzzy safety state is calculated based on the fuzzy probability theory. The procedure of the proposed method is shown in Figure 2.

Firstly, the computational dynamics model of the mechanism is constructed. The uncertainty sources in the model are identified. The epistemic uncertainty is represented by the fuzzy variables which are measured by possibility distributions. The aleatory uncertainty is represented by the random variables which are measured by probability distributions. Secondly, the Klir log-scale transformation is employed to unify the fuzzy variables and random variables. Then the series approximation method is conducted to transform the arbitrary random variables into the standard normal random variables. Thirdly, the sensitivity analysis is conducted to screen out the important uncertainty variables. The NIPC is constructed iteratively to determine the proper order of NIPC by comparing the moments with lower-order NIPC. Fourthly, the proper order NIPC is used to construct the motion error function. The membership function of the safety state is determined by experts and customers. Finally, the probability formula of the fuzzy event is solved numerically to calculate the kinematic reliability of the mechanism.

5. Case Study

A four-link mechanism consisting of the hydraulic actuator, rods, and joints as shown in Figure 3 is employed as our example.

The retractable mechanism is driven by the hydraulic actuator to make the device arm rotate to a specified angle. Then the device can switch between working position and stopping position. The kinematic reliability of the retractable mechanism is related to the rotating angle, which is affected greatly by the joint clearance and geometric tolerance.

5.1. Kinematics Modeling and Simulation. The computational dynamics model of the retractable mechanism is constructed. Meanwhile, the hydraulic control system with a PID controller is also built to be cosimulated with the computational dynamics model. And the kinetic outputs of the retractable mechanism can be obtained from the cosimulation. The structure of the cosimulation model is presented in Figure 4.

The time-varying cosimulation results of the mechanism at the nominal state during the retracted process are shown in Figures 5 and 6.

Because of the clearances in the joints, the mechanism would vibrate when it begins to retract. This phenomenon reflects on the drive force in Figure 5. And the drive force fluctuates during the initial 0.5 second. Then the drive force tends to be stabilized under the control of the PID controller. Figure 6 shows that the total operating time is 8.6054, and the rotating angle is 101.9966°, which is in the specified range between 101.2° and 102.8°.

Experiments have been conducted and practical kinetic data have been extracted from these experiments to verify and validate the kinematics model of the retractable mechanism.

5.2. NIPC-Based Mixed Uncertainty Quantification. According to the result of sensitivity analysis, the most important uncertain parameters for the kinematic reliability of the retractable mechanism are selected and their probability/possibility distributions are shown in Table 2.

"Length of the upper rod", "length of the actuator slider", and "clearance of the joint that links the actuator slider and the nether rod" are determined to follow a normal distribution according to the machining errors and assembly errors. "Coordinates X and Y of the position of the connector that links the device arm and the nether rod" are regarded as fuzzy variables. The reason can be summarized as follows. Uncertainties of these two position variables are determined

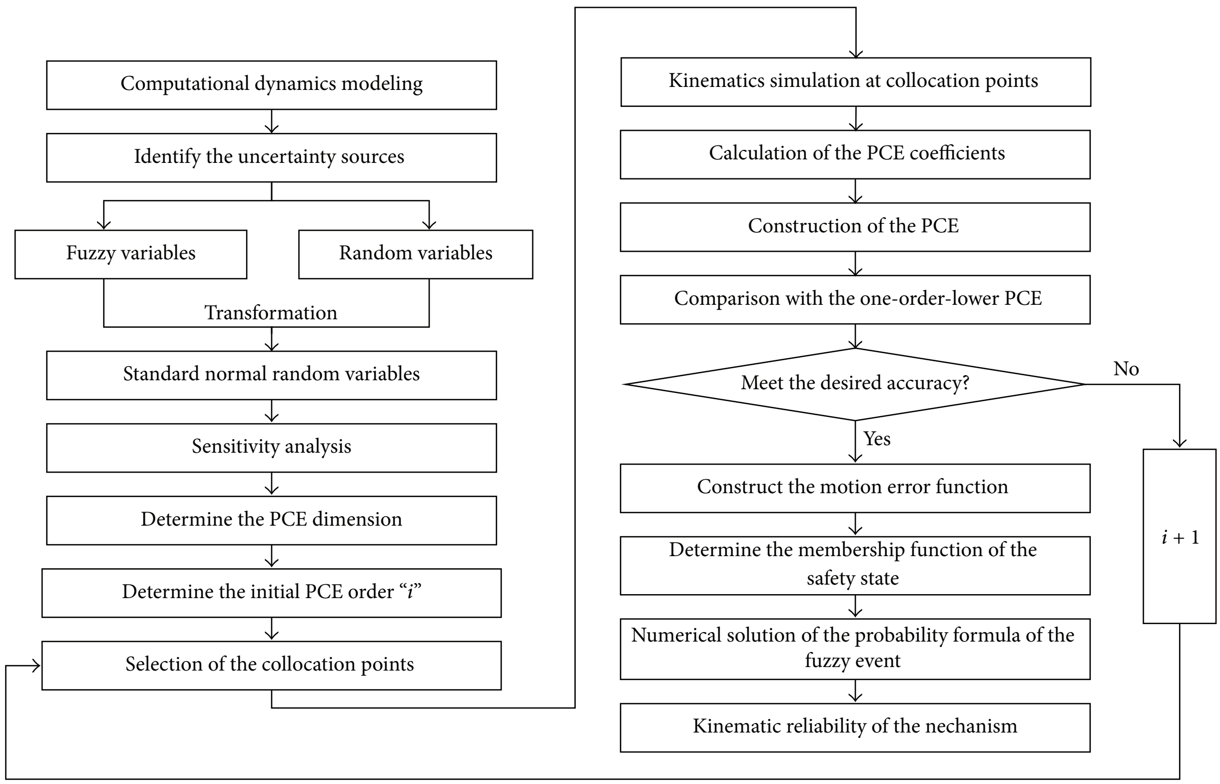

FIGURE 2: The procedure of the proposed NIPC-based kinematic reliability analysis method.

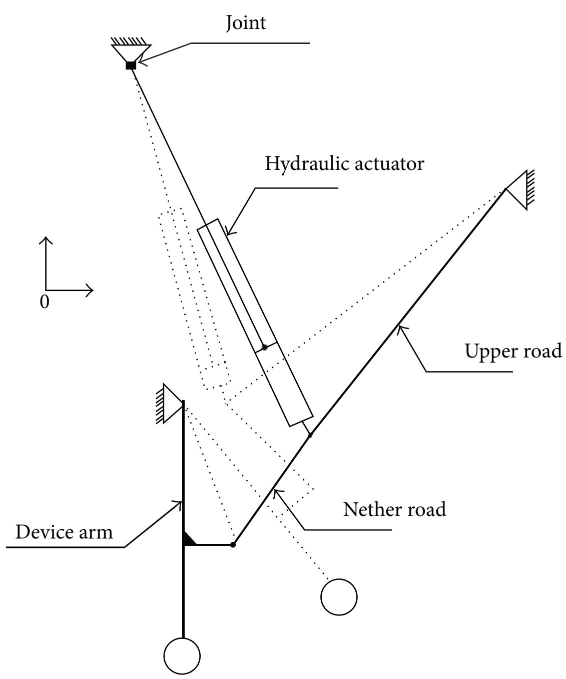

FIGURE 3: The schematic of the retractable mechanism.

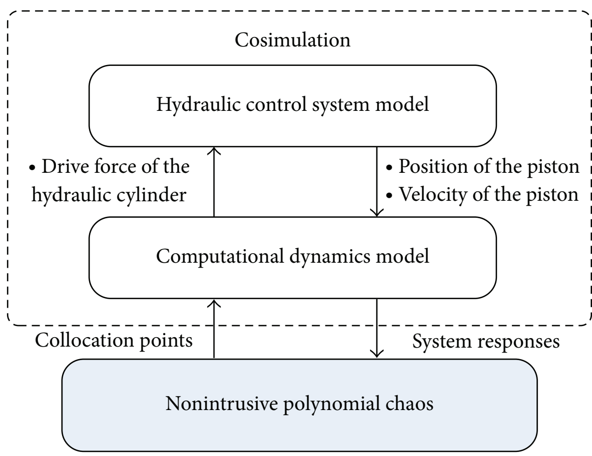

FIGURE 4: The procedure of the construction of NIPC.

by both the machining errors and the assembly errors of the device arm and the nether rod. The accurate position coordinates of the connector are difficult to measure. Meanwhile, because of the small production of the mechanism, scarcity data can be obtained to construct the probability distribution of these two uncertain variables. Probability theory is inapplicable in this case. Therefore, possibility theory is employed to measure the uncertainty with limited information of geometric parameters as well as the expertise. Coordinates X and Y of the position of the connector follow triangular possibility distribution.

Klir log-scale transformation is applied to unify the random and fuzzy variables. The proposed optimization algorithm is used to obtain the values of parameters α and β.

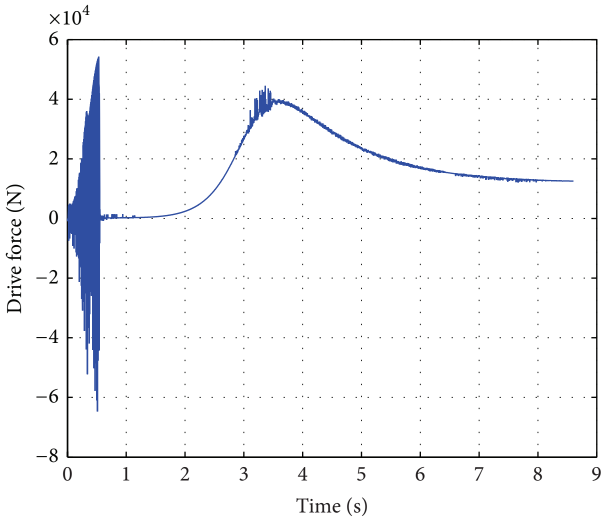

FIGURE 5: The time-varying drive force function.

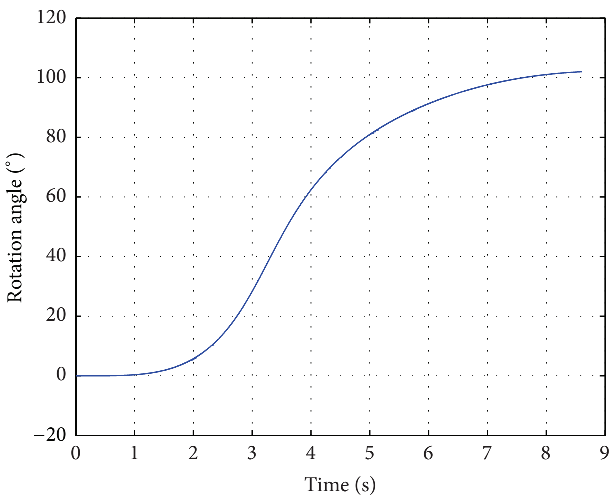

FIGURE 6: The time-varying rotating angle function.

The value accuracy of the Coordinates X and Y is 0.01 mm. Thus for the Coordinate X, the discrete values are presented as $X \in [850.00, 850.01, 850.02, \ldots, 870.00]$. The parameters are obtained as $\alpha = 0.3536$, $\beta = 522.3872$, and the transformed probability distribution is given by

$$p_X(x) = \begin{cases} \left[1.9143e^{-3} \cdot (0.1x - 85)\right]^{2.8281} & \\ & x = 850 : 0.01 : 860 \\ \left[1.9143e^{-3} \cdot (-0.1x + 87)\right]^{2.8281} & \\ & x = 860 : 0.01 : 870 \\ 0 & \text{otherwise.} \end{cases} \quad (28)$$

For the Coordinate Y, the discrete values are presented as $Y \in [-928.00, -927.99, -927.98, \ldots, -912.00]$. The parameters are obtained as $\alpha = 0.3512$, $\beta = 415.7603$, and the transformed probability distribution is given by

$$p_Y(x) = \begin{cases} \left[2.4052e^{-3} \cdot (0.125x + 116)\right]^{2.8474} & \\ & x = -928 : 0.01 : -920 \\ \left[2.4052e^{-3} \cdot (-0.125x - 114)\right]^{2.8474} & \\ & x = -920 : 0.01 : -912 \\ 0 & \text{otherwise.} \end{cases} \quad (29)$$

The possibility distributions and probability distributions of the Coordinate X and Coordinate Y are shown in Figures 7(a) and 7(b), respectively.

Since the Shannon entropy of the possibilistic variable and the probabilistic variable is preserved after the transformation, Klir log-scale transformation can generate a good transformation result.

The series approximation method is then used to convert the transformed random variables into standard normal random variables. The conversion formulas of the five parameters are shown in the last column of Table 2. The 3-order origin moment estimation errors of the approximate conversion formula of Coordinates X and Y are $1.1289e-5$ and $2.6097e-8$, respectively, which both meet the conversion accuracy.

The NIPC is conducted based on the Point-Collocation method. The 2-order and 3-order PCEs of the final rotating angle are built. As mentioned above, the number of collocation points that is twice more than the total number of the coefficients gives a better approximation. According to (5), the total numbers of coefficients of 2-order and 3-order PCEs are 21 and 56, respectively as there are five random variables. And the optimum numbers of collocation points are 42 and 112, respectively. Then the sets of standard normal random values are selected and converted into variable values of the computational dynamics model to obtain the final rotating angles through cosimulations. Equation (7) is applied to calculate the PCE coefficients. The 2-order and 3-order PCE formulas are shown in Appendix. After the construction of the PCEs, MCS with 10^6 samplings is performed on PCEs to obtain moments of the final rotation angle.

In Table 3, MCS with 10000 samplings is a benchmark for the comparison. The Kriging model and 2-order RSM are constructed based on 42 stochastic collocation points, which is the same amount of collocation points as the 2-order PCE. And it means that the RSM, Kriging model, and the 2-order PCE require the same amount of executions of the cosimulation. As shown in Table 3, the 2-order PCE is more accurate than the RSM and Kriging model on both the mean and the standard variance of the final rotating angle. This is especially true to the standard variance of the final rotating angle, where the relative error of the 2-order PCE is closed to 1/30 of the RSM, 1/5 of the Kriging model.

Meanwhile, the results of the 2-order PCE and the 3-order PCE are compared in Table 4. As mentioned above, 112 collocation points are required in the 3-order PCE, which is more than twice of that required by the 2-order PCE. It is shown in Table 4 that the relative error of the mean of the 3-order PCE is about 1/10 of the 2-order PCE. Its relative error of

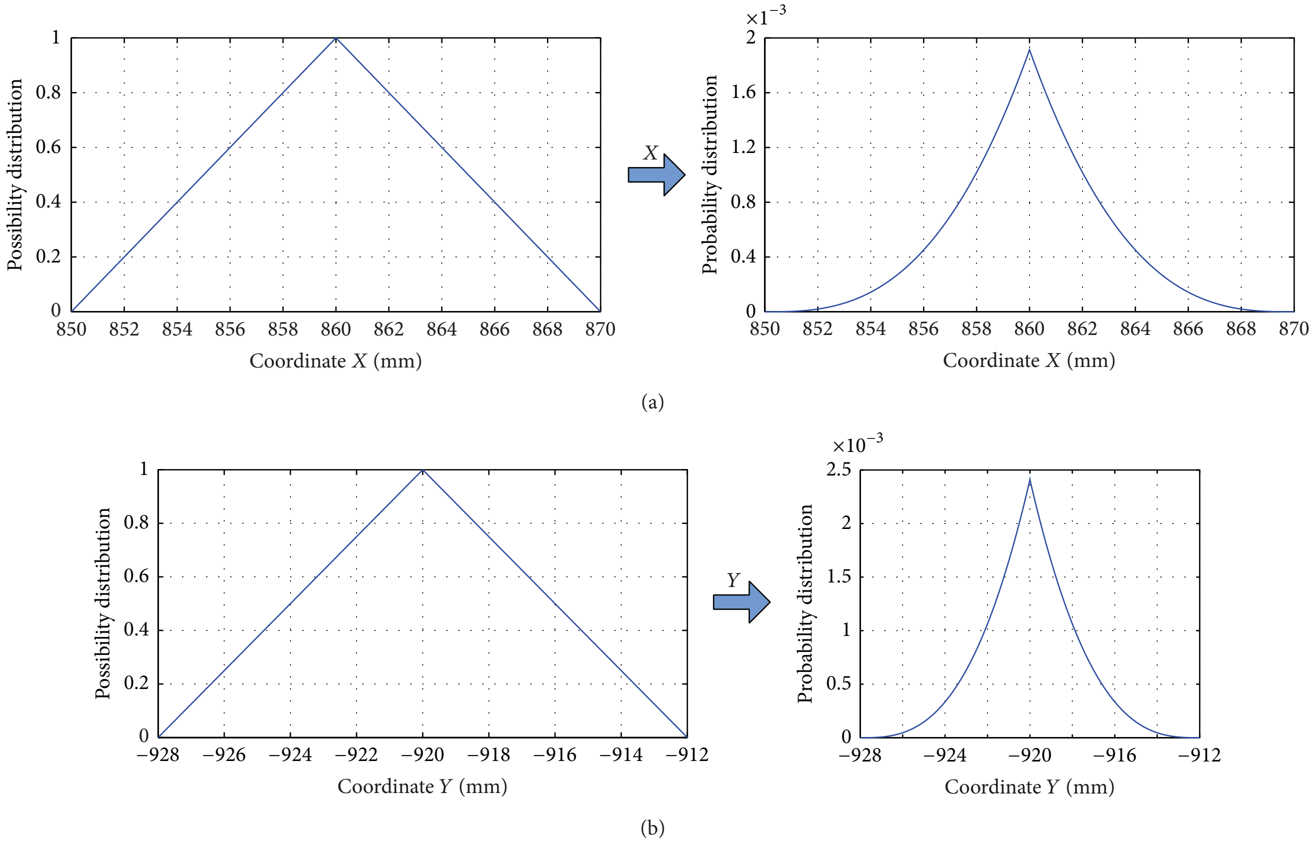

FIGURE 7: Possibility distribution functions and the corresponding transformed probability distribution functions: (a) possibility and transformed probability distribution functions of Coordinate X; (b) possibility and transformed probability distribution functions of Coordinate Y.

TABLE 2: Type, distribution, and conversion formula of the important uncertain parameters.

Parameters	Type of uncertainty	Probability/possibility distributions (mm)	Conversion formula
Length of the upper rod	Random	$N(1312, 3)$	$1312 + 3\xi_1$
Length of the actuator slider	Random	$N(1600, 3)$	$1600 + 3\xi_2$
Clearance of the joint that links the actuator slider and the nether rod	Random	$N(1.5e-2, 0.5e-2)$	$1.5 \times 10^{-2} + 0.5 \times 10^{-2}\xi_3$
Coordinate X of the position of the connector that links the device arm and the nether rod	Fuzzy	Triangular function $[850, 860, 870]$	$862.2361 - 2.2361\xi_4^2$
Coordinate Y of the position of the connector that links the device arm and the nether rod	Fuzzy	Triangular function $[-928, -920, -912]$	$-921.5152 + 1.5152\xi_5^2$

TABLE 3: Comparison of approximate results between the PCE and RSM.

Type of methods	Executions of cosimulations	Mean (°)	Standard variance	Relative error of mean (%)	Relative error of standard variance (%)
MCS	10000	101.9653	0.3682	/	/
RSM	42	101.9145	1.8285	0.0498	396.6051
Kriging	42	101.9114	0.0792	0.0529	78.4900
2-order PCE	42	101.9183	0.3143	0.0461	14.6388

Table 4: Comparison of approximate results between different order PCEs.

Type of methods	Executions of cosimulations	Mean (°)	Standard variance	Relative error of mean (%)	Relative error of standard variance (%)
MCS	10000	101.9653	0.3682	/	/
2-order PCE	42	101.9183	0.3143	0.0461	14.6388
3-order PCE	112	101.9603	0.3498	0.0049	4.9973

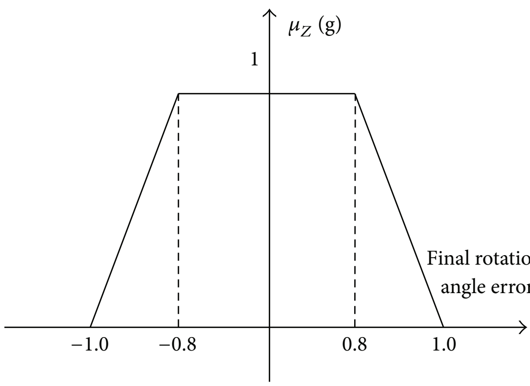

Figure 8: Membership function of the safety state of the mechanism.

the standard variance is closed to 1/3 of the 2-order PCE. The accuracy of PCE increases with its order obviously. But higher order PCE requires more collocation points which means that more executions of simulations are needed. Thus a tradeoff should be made to balance the efficiency and accuracy.

5.3. Kinematic Reliability Analysis Based on Fuzzy Probability Theory. The failure criterion of the mechanism is related to the final rotating angle. According to the mission requirements and expertise, the membership function of the safety state of the mechanism is determined as a trapezoid function, as shown in Figure 8.

The formula of the membership function is written as follows:

$$\mu_Z(g) = \begin{cases} 5g+5 & -1 < g < -0.8 \\ 1 & -0.8 \le g \le 0.8 \\ -5g+5 & 0.8 < g < 1 \\ 0 & \text{otherwise.} \end{cases} \tag{30}$$

The algorithm presented in Section 4.2 is executed, and in total, 10^6 samplings are employed for RSM and Kriging, as well as 2-order and 3-order PCEs to calculate the kinematic reliability. The results are compared with the MCS, RSM, and Kriging method in Table 5.

The kinematic reliability in Table 5 demonstrates that the proposed NIPC-based method is able to quantify the mixed uncertainty and compute the kinematic reliability for the mechanism with fuzzy and random variables as well as fuzzy states. Meanwhile, the comparisons in Tables 3 and 5 show that PCE is more accurate than RMS and Kriging method with the same number of collocation points. Thus it is demonstrated that the proposed NIPC-based kinematic reliability analysis method has high computational accuracy and efficiency.

Table 5: Kinematic reliability calculated by the PCE, RSM, and MCS.

Type of methods	Executions of cosimulations	Kinematic reliability with fuzzy safety state	Relative error with MCS (%)
MCS	10000	0.9823	/
RSM	42	0.8723	11.1982
Kriging	42	0.9967	1.4669
2-order PCE	42	0.9874	0.5192
3-order PCE	112	0.9849	0.2647

6. Conclusion

In this paper, the problem of mixed uncertainty quantification in the analysis of kinematic reliability is addressed. For this purpose, the NIPC-based method is extended to tackle with the coexistence of the fuzzy and random variables in the mechanisms through the Klir log-scale transformation. Meanwhile, the fuzzy states of the mechanisms are also considered by the fuzzy probability theory. Corresponding procedure and algorithm are developed to obtain the kinematic reliability. We use the retractable mechanical system as an example to show that the proposed NIPC-based method is able to evaluate the kinematic reliability under both fuzzy and random variables as well as fuzzy failure/safety state. The results are more accurate and efficient than the RSM and Kriging method. The accuracy of the proposed NIPC-based method would increase with the PCE order. The proper order can be obtained through the comparison of the accuracy with the lower-order PCE until the difference satisfies the predetermined requirement.

Appendix

During the construction of the 2-order and 3-order PCEs, the polynomial would be abandoned as its coefficient value is less than 0.0001. The 2-order PCE of the final rotating angle is given by

$$A_2 = 101.9183 - 0.1382\xi_1 - 0.2586\xi_2 - 0.0002\xi_3 + 0.0003\xi_4 + 0.0002\xi_5 - 0.0799\left(\xi_1^2 - 1\right)$$

$$+ 0.0008\left(\xi_2^2-1\right)+0.0090\left(\xi_3^2-1\right) - 0.0035\left(\xi_4^2-1\right)-0.0002\left(\xi_5^2-1\right) - 0.0001\xi_1\xi_2+0.0001\xi_1\xi_3+0.0001\xi_1\xi_4 + 0.0004\xi_1\xi_5-0.0001\xi_2\xi_3-0.0001\xi_2\xi_4 + 0.0004\xi_2\xi_5+0.0001\xi_3\xi_4-0.0001\xi_4\xi_5. \tag{A.1}$$

And the 3-order PCE of the final rotating angle is given by

$$\begin{aligned} A_3 = {} & 101.9603-0.2058\xi_1-0.2584\xi_2-0.0003\xi_3 \\ & +0.0003\xi_4-0.0001\xi_5-0.0653\left(\xi_1^2-1\right) \\ & +0.0011\left(\xi_2^2-1\right)+0.0011\left(\xi_3^2-1\right) \\ & -0.0032\left(\xi_4^2-1\right)+0.0002\left(\xi_5^2-1\right) \\ & +0.0276\left(\xi_1^3-3\xi_1\right)-0.0001\left(\xi_2^3-3\xi_2\right) \\ & -0.0002\left(\xi_4^3-3\xi_4\right)-0.0003\xi_1\xi_2+0.0001\xi_1\xi_4 \\ & -0.0001\xi_2\xi_3-0.0001\xi_2\xi_5+0.0001\xi_3\xi_4 \\ & +0.0001\left(\xi_1\xi_2^2-\xi_1\right)-0.0001\left(\xi_1\xi_3^2-\xi_1\right) \\ & +0.0003\left(\xi_1\xi_4^2-\xi_1\right)-0.0001\left(\xi_1\xi_5^2-\xi_1\right) \\ & -0.0002\left(\xi_2\xi_1^2-\xi_2\right)+0.0001\left(\xi_3\xi_2^2-\xi_3\right) \\ & +0.0001\left(\xi_5\xi_2^2-\xi_5\right)-0.0001\xi_1\xi_2\xi_5 \\ & +0.0001\xi_1\xi_4\xi_5-0.0001\xi_2\xi_4\xi_5. \end{aligned} \tag{A.2}$$

Abbreviations

Acronyms

MCS: Monte Carlo simulation
NIPC: NonIntrusive polynomial chaos
PCE: Polynomial chaos expansion
PDF: Probability density functions
RSM: Response surface method
SOP: Second-order probability
SQP: Sequential quadratic programming.

Notations

$G(\boldsymbol{\xi})$: System response
a_i: The ith coefficient of the PCE
$\Gamma_n(\xi_{i_1},\ldots,\xi_{i_n})$: The selected polynomial basis function
ξ_{i_1}: The random variable with specific distribution
p: The order of the PCE
n: The total number of random variables
N_a: The total number of coefficients of the PCE
q: The total number of the sets of collocation points
$\boldsymbol{\xi}$: The vector of the standard normal random variables
$\mathbf{v}$: The vector of fuzzy variables
$p(s_i)$: The probability of the element s_i
$\pi(s_i)$: The possibility of the element s_i
α: The parameter of the Klir log-scale transformation
β: The parameter of the Klir log-scale transformation
$\phi(\mathbf{x},\mathbf{v})$: The actual motion output of the mechanism
ϕ_d: The desired motion output of the mechanism
R_k: The kinematic reliability.

Conflict of Interests

The authors declare that there is no conflict of interests regarding the publication of this paper.

Acknowledgment

This work was funded by National Natural Science Foundation of China (NSFC: 61304218).

References

[1] P. Eberhard and W. Schiehlen, "Computational dynamics of multibody systems: history, formalisms, and applications," *Journal of Computational and Nonlinear Dynamics*, vol. 1, no. 1, pp. 3–12, 2006.

[2] P. K. Bhatti, *Probabilistic modeling and optimal design of robotic manipulators [dissertation]*, Purdue University, 1989.

[3] S. S. Rao and P. K. Bhatti, "Probabilistic approach to manipulator kinematics and dynamics," *Reliability Engineering and System Safety*, vol. 72, no. 1, pp. 47–58, 2001.

[4] J. Zhang and X. Du, "Time-dependent reliability analysis for function generator mechanisms," *Journal of Mechanical Design*, vol. 133, no. 3, Article ID 031005, 2011.

[5] M. S. Eldred, "Recent advances in non-intrusive polynomial chaos and stochastic collocation methods for uncertainty analysis and design," in *Proceedings of the 50th AIAA/ASME/ASCE/AHS/ASC Structures, Structural Dynamics and Materials Conference*, Palm Springs, Calif, USA, May 2009.

[6] D. Xiu and G. Em Karniadakis, "The Wiener-Askey polynomial chaos for stochastic differential equations," *SIAM Journal on Scientific Computing*, vol. 24, no. 2, pp. 619–644, 2003.

[7] S. Hosder, R. W. Walters, and M. Balch, "Efficient sampling for non-intrusive polynomial chaos applications with multiple uncertain input variables," in *Proceedings of the 48th AIAA/ASME/ASCE/AHS/ASC Structures, Structural Dynamics, and Materials Conference*, Number AIAA-2007-1939, pp. 2946–2961, Honolulu, Hawaii, USA, April 2007.

[8] W. Yao, X. Chen, W. Luo, M. van Tooren, and J. Guo, "Review of uncertainty-based multidisciplinary design optimization methods for aerospace vehicles," *Progress in Aerospace Sciences*, vol. 47, no. 6, pp. 450–479, 2011.

[9] M. Sallak, W. Schön, and F. Aguirre, "Extended component importance measures considering aleatory and epistemic

uncertainties," *IEEE Transactions on Reliability*, vol. 62, no. 1, pp. 49–65, 2013.

[10] S. Destercke and M. Sallak, "An extension of universal generating function in multi-state systems considering epistemic uncertainties," *IEEE Transactions on Reliability*, vol. 62, no. 2, pp. 504–514, 2013.

[11] A. Monti, F. Ponci, and M. Valtorta, "Extending polynomial chaos to include interval analysis," *IEEE Transactions on Instrumentation and Measurement*, vol. 59, no. 1, pp. 48–55, 2010.

[12] N. Wiener, "The homogeneous chaos," *American Journal of Mathematics*, vol. 60, no. 4, pp. 897–936, 1938.

[13] G. T. Buzzard, "Global sensitivity analysis using sparse grid interpolation and polynomial chaos," *Reliability Engineering and System Safety*, vol. 107, pp. 82–89, 2012.

[14] Z. Hu, H. Li, X. Du, and K. Chandrashekhara, "Simulation-based time-dependent reliability analysis for composite hydrokinetic turbine blades," *Structural and Multidisciplinary Optimization*, vol. 47, no. 5, pp. 765–781, 2013.

[15] X. Zhang, Z. Hu, and X. Du, "Probabilistic inverse simulation and its application in vehicle accident reconstruction," *Journal of Mechanical Design*, vol. 135, no. 12, Article ID 121006, 2013.

[16] R. Walters, "Towards stochastic fluid mechanics via polynomial chaos," in *Proceedings of the 41 st AIAA Aerospace Sciences Meeting & Exhibit*, Reno, Nev, USA, 2003.

[17] S. Hosder, R. W. Walters, and R. Perez, "A non-intrusive polynomial chaos method for uncertainty propagation in CFD simulations," in *Proceedings of the 44th AIAA Aerospace Sciences Meeting 2006*, pp. 10649–10667, January 2006.

[18] Y. Ping, Z. YiFang, and Z. Ji, "A systematic design and evaluation method for output characteristics of epicyclic gear trains," *Mechanism and Machine Theory*, vol. 38, no. 1, pp. 43–52, 2003.

[19] E. Nikolaidis, S. Chen, H. Cudney, R. T. Haftka, and R. Rosca, "Comparison of probability and possibility for design against catastrophic failure under uncertainty," *Journal of Mechanical Design*, vol. 126, no. 3, pp. 386–394, 2004.

[20] L. A. Zadeh, "Fuzzy sets as a basis for a theory of possibility," *Fuzzy Sets and Systems*, vol. 100, no. 1, pp. 9–34, 1999.

[21] Y. Ding, M. J. Zuo, A. Lisnianski, and Z. Tian, "Fuzzy multi-state systems: general definitions, and performance assessment," *IEEE Transactions on Reliability*, vol. 57, no. 4, pp. 589–594, 2008.

[22] M. Sallak, C. Simon, and J. Aubry, "A fuzzy probabilistic approach for determining safety integrity level," *IEEE Transactions on Fuzzy Systems*, vol. 16, no. 1, pp. 239–248, 2008.

[23] S. Bugajski, "Fundamentals of fuzzy probability theory," *International Journal of Theoretical Physics*, vol. 35, no. 11, pp. 2229–2244, 1996.

[24] P. Smets, "Constructing the pignistic probability function in a context of uncertainty," *Uncertainty in Artificial Intelligence*, vol. 5, pp. 29–40, 1990.

[25] G. J. Klir, "A principle of uncertainty and information invariance," *International Journal of General Systems*, vol. 17, no. 2-3, pp. 249–275, 1990.

[26] M. Oussalah, "On the probability/possibility transformations: a comparative analysis," *International Journal of General Systems*, vol. 29, no. 5, pp. 671–718, 2000.

[27] Z. Lu and J. Sun, "General response surface reliability analysis for fuzzy-random uncertainty both in basic variables and in state variables," *Chinese Journal of Aeronautics*, vol. 18, no. 2, pp. 116–121, 2005.

[28] R. R. Yager, "Element selection from a fuzzy subset using the fuzzy integral," *IEEE Transactions on Systems, Man and Cybernetics*, vol. 23, no. 2, pp. 467–477, 1993.

[29] J. F. Geer and G. J. Klir, "A mathematical analysis of information-preserving transformations between probabilistic and possibilistic formulations of uncertainty," *International Journal of General Systems*, vol. 20, no. 2, pp. 143–176, 1992.